4-1994

Theoretical Study of Pseudorotation of Pentacoordinated Silicon Anions: SiH5-nXn- (X = F, Cl)

Theresa Lynn Windus
Iowa State University, twindus@iastate.edu

Mark S. Gordon
Iowa State University, mgordon@iastate.edu

Larry P. Davis
Air Force Office of Scientific Research

Larry W. Burggraf
Air Force Institute of Technology

Theoretical Study of Pseudorotation of Pentacoordinated Silicon Anions: SiH5-nXn- (X = F, Cl)

Abstract
A thorough ab initio investigation of the pseudorotation of the pentacoordinated silicon anions SiHs...Xn- (X = F, Cl; n = 0-5) is reported. The minima and maxima of each of the systems under consideration are characterized and intrinsic reaction coordinate (IRC) calculations are performed to connect the maxima with corresponding minima. These systems are compared to the Berry pseudorotation mechanism and earlier calculations on these systems.

Disciplines
Chemistry

Comments
This article is from *Journal of the American Chemical Society* 116 (1994): 3568. doi:10.1021/ja00087a050.

Theoretical Study of Pseudorotation of Pentacoordinated Silicon Anions: $SiH_{5-n}X_n^-$ (X = F, Cl)

Theresa L. Windus,† Mark S. Gordon,*,† Larry P. Davis,‡ and Larry W. Burggraf§

Contribution from the Department of Chemistry, Iowa State University, Ames, Iowa 50011, Air Force Office of Scientific Research, Bolling Air Force Base, D.C. 20332, and Air Force Institute of Technology, Engineering Physics Department, Wright-Patterson Air Force Base, Ohio 45433

Received November 4, 1993. Revised Manuscript Received February 7, 1994®

Abstract: A thorough *ab initio* investigation of the pseudorotation of the pentacoordinated silicon anions $SiH_{5-n}X_n^-$ (X = F, Cl; n = 0–5) is reported. The minima and maxima of each of the systems under consideration are characterized and intrinsic reaction coordinate (IRC) calculations are performed to connect the maxima with corresponding minima. These systems are compared to the Berry pseudorotation mechanism and earlier calculations on these systems.

Introduction

The existence and stabilities of pentacoordinated silicon anions of the type $SiX_nY_{5-n}^-$ play a major role in the mechanism for nucleophilic displacement reactions occurring at silicon and the resulting stereochemistry of these displacements.[1] We have been investigating these issues for the last several years[2-4] at both the semiempirical and *ab initio* levels, and our previous work has been quite successful in predicting which pentacoordinated species should be present in gas-phase reactions of this type.[2b]

In this paper we systematically explore the trends in the relative energetics for the various stationary points (both stable and otherwise) on the potential energy surfaces of the series $SiH_nX_{5-n}^-$, X = F or Cl. In particular, we compare our results with the early *ab initio* work of Willhite and Spialter[5] (WS), who conducted studies on the $SiH_nX_{5-n}^-$ series that modeled the electronegative atom "X" by increasing the hydrogen nuclear charge. Our results, coupled with previous theoretical and experimental work, offer new insights into the stereochemical structure of pentacoordinated silicon compounds. This in turn will have a strong impact on silicon-centered nucleophilic substitution reactions based on the nature of the Berry pseudorotational[6] potential energy surfaces of the pentacoordinated silicon intermediates.

The rest of the paper is organized in the following manner. First the computational methods used will be discussed. Then, the results and discussion for each individual system will be presented, followed by the conclusions.

Computational Methods

All *ab initio* structure, energy, and frequency calculations were performed with locally modified versions of GAUSSIAN88,[7] GAUSSIAN90,[8] or the San Diego Supercomputer Center version of GAUSSIAN92.[9] Structures were obtained at the restricted Hartree–Fock RHF/6-31G(d)[10] (level A), the RHF/6-31++G(d,p)[11] (level B), and the second-order Moller–Plesset[12] perturbation MP2/6-31++G(d,p) (level C) levels of theory. Level A was used to probe the surface of the species in question. Levels B and C were used to explore the importance of using diffuse functions and correlation to determine the structures of these species. As will be discussed later, several of these species require the use of the higher levels of theory to obtain even qualitatively correct results. The molecules were restricted to the appropriate point group symmetry during the optimization step. The symmetries used are noted in the figures.

Energy information was obtained at each of the optimization levels. In addition, fourth-order Moller–Plesset[13] perturbation (MP4) energies were calculated at each of the optimization levels using the 6-31++G-(d,p) basis set.

Second derivatives of the energy with respect to the nuclear coordinates were calculated at each stationary point at all levels of theory used for geometry determination. The Cartesian force constant matrix (hessian) was diagonalized to determine frequencies and zero-point energies and to verify that minima and transition states had zero and one imaginary frequency, respectively.

Intrinsic reaction coordinate[14] (IRC) calculations were performed with the GAMESS[15] *ab initio* program to "connect" maxima with corresponding minima. The specific methods used were Euler with stabilization (ES2),[16] fourth-order Runge–Kutta (RK4),[17] and second-order Gonzalez–

* Author to whom correspondence should be addressed.
† Iowa State University.
‡ Bolling Air Force Base.
§ Wright-Patterson Air Force Base.
® Abstract published in *Advance ACS Abstracts,* April 1, 1994.

(1) (a) Corriu, R. J. P.; Guerin, C. *J. Organomet. Chem.* **1980**, *198*, 231. (b) Corriu, R. J. P.; Guerin, C. *Adv. Organomet. Chem.* **1982**, *20*, 265. (c) Eisch, J. J.; Chiu, C. S. *J. Organomet. Chem.* **1988**, *358*, C1–C5. (d) Mislow, K. *Acc. Chem. Res.* **1970**, *3*, 321–331.

(2) (a) Gordon, M. S.; Davis, L. P.; Burggraf, L. W.; Damrauer, R. *J. Am. Chem. Soc.* **1986**, *108*, 7889–93. (b) Damrauer, R.; Burggraf, L. W.; Davis, L. P.; Gordon, M. S. *J. Am. Chem. Soc.* **1988**, *110*, 6601–6606. (c) Davis, L. P.; Burggraf, L. W.; Gordon, M. S. *J. Am. Chem. Soc.* **1988**, *110*, 3056–3062. (d) Davis, L. P.; Burggraf, L. W.; Gordon, M. S. *Int. J. Quantum Chem.* **1992**, *44*, 691–698. (e) Gordon, M. S.; Carroll, M. T.; Davis, L. P.; Burggraf, L. W. *Comp. Mat. Sci.*, **1993**, *1*, 161–168.

(3) Gordon, M. S.; Windus, T. L.; Burggraf, L. W.; Davis, L. P. *J. Am. Chem. Soc.* **1990**, *112*, 7167–7171.

(4) Windus, T. L.; Gordon, M. S.; Burggraf, L. W.; Davis, L. P. *J. Am. Chem. Soc.* **1991**, *113*, 4356–4357.

(5) Willhite, D. L.; Spialter, L. *J. Am. Chem. Soc.* **1973**, *95*, 2100–04.

(6) (a) Berry, R. S. *J. Chem. Phys.* **1960**, *32*, 933–938. (b) Mislow, K. *Acc. Chem. Res.* **1970**, *3*, 321.

(7) Frisch, M. J.; Head-Gordon, M.; Schlegel, H. B.; Raghavachari, K.; Binkley, J. S.; Gonzalez, C.; DeFrees, D. J.; Fox, D. J.; Whiteside, R. A.; Seeger, R.; Melius, C. F.; Baker, J.; Martin, R. L.; Kahn, L. R.; Stewart, J. J. P.; Fluder, E. M.; Topiol, S.; Pople, J. A. Gaussian, Inc., Pittsburgh, PA.

(8) Frisch, M. J.; Head-Gordon, M.; Trucks, G. W.; Foresman, J. B.; Schlegel, H. B.; Raghavachari, K.; Robb, M.; Binkley, J. S.; Gonzalez, C.; Defrees, D. J.; Fox, D. J.; Whiteside, R. A.; Seeger, R.; Melius, C. F.; Baker, J.; Martin, R. L.; Kahn, L. R.; Stewart, J. J. P.; Topiol, S.; Pople, J. A. Gaussian, Inc., Pittsburgh, PA, 1990.

(9) Frisch, M. J.; Trucks, G. W.; Head-Gordon, M.; Gill, P. M. W.; Wong, M. W.; Foresman, J. B.; Johnson, B. G.; Schlegel, H. B.; Robb, M. A.; Foresman, J. B.; Johnson, B. G.; Schlegel, H. B.; Robb, M. A.; Replogle, E. S.; Gomperts, R.; Andres, J. L.; Raghavachari, K.; Binkley, J. S.; Gonzalez, C.; Martin, R. L.; Fox, D. J.; Defrees, D. J.; Baker, J.; Stewart, J. J. P.; Pople, J. A. Gaussian, Inc., Pittsburgh, PA, 1992.

(10) (a) Hehre, W. J.; Ditchfield, R.; Pople, J. A. *J. Chem. Phys.* **1972**, *56*, 2257–2261. (b) Francl, M. M.; Pietro, W. J.; Hehre, W. J.; Binkley, J. S.; Gordon, M. S.; DeFrees, D. J.; Popel, J. A. *J. Chem. Phys.* **1982**, *77*, 3654–3665. (c) Gordon, M. S. *Chem. Phys. Lett.* **1980**, *76*, 163–168. (d) Ditchfield, R.; Hehre, W. J.; Pople, J. A. *J. Chem. Phys.* **1971**, *54*, 724–728. (e) Hariharan, P. C.; Pople, J. A. *Theor. Chim. Acta* **1973**, *28*, 213–222.

(11) Frisch, M. J.; Pople, J. A.; Binkley, J. S. *J. Chem. Phys.* **1984**, *80*, 3265.

(12) (a) Carsky, P.; Hess, B. A.; Schaad, L. J. *J. Comp. Chem.* **1984**, *5*, 280–287. (b) Pople, J. A.; Binkley, J. S.; Seeger, R. *Int. J. Quantum Chem.* **1976**, *S10*, 1–19.

(13) Krishnan, R.; Frisch, M. J.; Pople, J. A. *J. Chem. Phys.* **1980**, *72*, 4244.

(14) Fukui, K. *Acc. Chem. Res.* **1981**, *14*, 363.

(15) Schmidt, M. W.; Baldridge, K. K.; Boatz, J. A.; Elber, S. T.; Gordon, M. S.; Jensen, J. H.; Koseki, S.; Matsunaga, N.; Nguyen, K. A.; Su, S.; Windus, T. L.; Dupuis, M.; Montgomery, J. A., Jr. *J. Comput. Chem.*, accepted for publication.

0002-7863/94/1516-3568$04.50/0

Table 1. MP4/6-31++G(d,p)//MP2/6-31++G(d,p) Energetics of the $SiX_nY_{4-n} + Y^- \rightarrow SiX_nY_{5-n}^-$ Reactions (in kcal/mol)

	ΔE	ΔH^a
SiH_5^-		
$SiH_4 + H^-$	−18.1	−15.8
SiH_4F^-		
$SiH_4 + F^-$	−31.5	−30.6
$SiH_3F + H^-$	−46.0	−42.5
SiH_4Cl^-		
$SiH_4 + Cl^-$	−5.2	−4.6
$SiH_3Cl + H^-$	−61.2	−57.3
$SiH_3F_2^-$		
$SiH_3F + F^-$	−52.1	−51.0
$SiH_2F_2 + H^-$	−61.3	−57.2
$SiH_3Cl_2^-$		
$SiH_3Cl + Cl^-$	−22.4	−21.7
$SiH_2Cl_2 + H^-$	−76.9	−72.4
$SiH_2F_3^-$		
$SiH_2F_2 + F^-$	−58.9	−54.4
$SiHF_3 + H^-$	−67.1	−62.7
$SiH_2Cl_3^-$		
$SiH_2Cl_2 + Cl^-$	−23.4	−22.9
$SiHCl_3 + H^-$	−77.7	−73.0
$SiHF_4^-$		
$SiHF_3 + F^-$	−65.2	−64.3
$SiF_4 + H^-$	−78.3	−73.7
$SiHCl_4^-$		
$SiHCl_3 + Cl^-$	−22.8	−22.5
$SiCl_4 + H^-$	−78.1	−76.4
SiF_5^-		
$SiF_4 + F^-$	−73.4	−72.3
$SiCl_5^-$		
$SiCl_4 + Cl^-$	−22.2	−21.9

[a] Includes zero-point vibrational energy corrections.

Schlegel (GS2).[18] ES2 and RK4 were used before the new addition of GS2 to GAMESS. We have found that the GS2 method is much more cost effective than the other two methods for IRCs, since larger step sizes can be used while still having an IRC that is converged. All IRCs are calculated at level B unless otherwise specified.

The notation level2/basis2//level1/basis1 is used throughout this paper to represent energetics calculated at level2 using basis2 at the structure optimized at level1 using basis1.

Results and Discussion

Reactants. All of the reactants of the reaction

$$SiX_nY_{4-n} + Y^- \rightarrow SiX_nY_{5-n}^- \qquad (1)$$

where X, Y = H, F, or Cl, have been optimized within the appropriate point group symmetry at the C level of theory. The geometric information for these structures is available as supplementary material. The energetics for these systems at the MP4/6-31++G(d,p)//MP2/6-31++G(d,p) level are given in Table 1.

Interestingly, the exothermicities for these reactions are, in general, quite large. Indeed, it was demonstrated in a previous paper that many of the pentacoordinated species that are predicted to be quite stable can be detected in flowing afterglow.[2b]

Investigations are currently in progress to determine the extent that the energy gained upon formation of the pentacoordinated anion can be transferred into the pseudorotational motion.[19] Most of the pentacoordinated isomers are below the dissociation limits calculated here; however, a few of them are not. These particular systems will be discussed in the sections to follow.

SiH_5^-. We have previously reported[3] our results for this system. The structures in Figure 1 and energetics in Table 2 are included for completeness. As reported in our previous study, the results agree well with those of other workers.[5,20] This system follows the typical Berry pseudorotational process[6] which is shown in Scheme 1.

Scheme 1. Typical Berry Pseudorotational Process for SiX_5^-

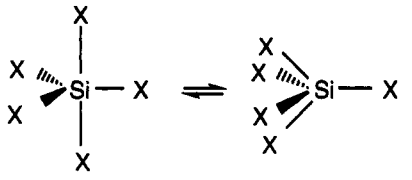

1 2

The (local minimum) trigonal bipyramid (TB), **1**, will pseudorotate to an equivalent structure (assuming that all ligands are equivalent) through the square pyramidal (SPY) transition state (TS), **2**. This is accomplished by "freezing" one of the equatorial ligands as the pivot atom. Then the other two equatorial ligands move away from each other to become axial and the axial ligands move toward each other to become equatorial.

The IRC for this system has been calculated to definitively prove the reaction pathway. The RK4 method was used at the MP2/6-31G(d) level for this purpose.[3] Since the reaction of $SiH_4 + H^-$ produces 15.8 kcal/mol of energy, we are currently investigating through the use of semiclassical trajectories how much of this energy can be transferred into the pseudorotational motion and if there is any mode specificity in the reaction.

SiH_4F^-. We have also previously reported[4] our results on the SiH_4F^- system. The structures in Figure 2, geometries in Table 3, and energetics in Table 2 are included here for completeness. This system, unlike the SiH_5^- system, displays characteristics that are much different from those of the "typical" Berry pseudorotation. Scheme 2 represents the expected Berry pseudorotation mechanism for a monosubstituted system.

Our previous work showed that at levels B and C the structures corresponding to the F equatorial in the TB (**2** in Scheme 2) and the F basal in the SPY (**3** in Scheme 2) have coalesced into one structure: a TS (**2** in Figure 2).[4] The pseudorotational process is therefore much different than would be expected.

Scheme 2. Expected Berry Pseudorotational Mechanism for SiH_4X^-

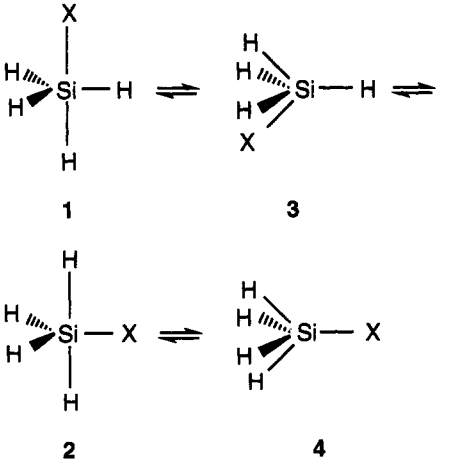

1 3

2 4

(16) (a) Ishida, K.; Morokuma, K.; Kormornicki, A. *J. Chem. Phys.* **1977**, *66*, 2153. (b) Schmidt, M. W.; Gordon, M. S.; Dupuis, M. *J. Am. Chem. Soc.* **1985**, *107*, 2585.

(17) Baldridge, K. K.; Gordon, M. S.; Steckler, R.; Truhlar, D. G. *J. Phys. Chem.* **1989**, *93*, 5107.

(18) (a) Gonzalez, C.; Schlegel, H. B. *J. Phys. Chem.* **1990**, *94*, 5523. (b) Gonzalez, C.; Schlegel, H. B. *J. Phys. Chem.* **1991**, *95*, 5853.

(19) Bintz, K.; Thompson, D. L.; Windus, T. L.; Gordon, M. S. Work in progress.

(20) (a) Burggraf, L. W.; Davis, L. P.; Gordon, M. S. *Top. Phys. Organomet. Chem.* **1989**, *3*, 75. (b) Reed, A. E.; Schleyer, P. R. *Chem. Phys. Lett.* **1987**, *133*, 553–561. (c) Frolov, Y. L.; Shevchenko, S. G.; Voronkov, M. G. *J. Organomet. CHem.* **1985**, *292*, 159–166. (d) Vitkovskaya, N. M.; Mantsivoda, V. B.; Moskovkaya, T. E.; Voronkov, M. G. *Int. J. Quantum Chem.* **1980**, *17*, 299–305. (e) Keil, F.; Ahlrichs, R. *Chem. Phys.* **1975**, *8*, 384–390.

Table 2. Relative Energies (in kcal/mol) (The Values in Parentheses Include Zero-Point Energies; the RHF Frequencies Are Scaled by 0.89)

structure	MP4/6-31++G(d,p)//RHF/6-31G(d)[a]		MP4/6-31++G(d,p)//RHF/6-31++G(d,p)[a]		MP4/6-31++G(d,p)//MP2/6-31++G(d,p)[a]	
SiH_5^-						
1					0.0	(0.0)
2					2.5	(2.2)
SiH_4F^-						
1	0.0	(0.0)	0.0	(0.0)	0.0	(0.0)
2	7.7	(7.4)	8.1	(7.5)	7.7	(7.2)
3	7.1	(6.6)				
4	22.2	(21.3)	23.2	(22.1)	23.2	(22.0)
SiH_4Cl^-						
1	0.0	(0.0)	0.0	(0.0)	0.0	(0.0)
4	33.4	(32.2)	33.2	(31.9)	33.4	(32.1)
$SiH_3F_2^-$						
1	0.0	(0.0)	0.0	(0.0)	0.0	(0.0)
2	9.0	(8.7)	9.5	(9.0)	9.2	(8.9)
3	11.6	(11.3)	13.2	(12.7)	12.8	(12.5)
4	11.1	(10.7)				
5	11.2	(10.6)	11.9	(11.2)	11.7	(11.1)
6	16.2	(15.5)	16.9	(16.0)	16.7	(15.9)
$SiH_3Cl_2^-$						
1	0.0	(0.0)	0.0	(0.0)	0.0	(0.0)
2	14.9	(14.5)			14.8	(14.5)
3						
4	14.4	(13.9)				
5	20.3	(19.8)	20.2	(19.7)	20.4	(19.9)
6	23.3	(22.7)	23.2	(22.6)	23.4	(22.7)
$SiH_2F_3^-$						
1	0.0	(0.0)	0.0	(0.0)	0.0	(0.0)
2	6.1	(6.2)	5.7	(5.8)	5.6	(5.7)
3	7.3	(7.1)	7.4	(7.1)	7.1	(6.9)
4	6.1	(6.1)	5.8	(5.9)	5.7	(5.7)
5	11.3	(10.7)	11.1	(10.4)	10.9	(10.3)
6	6.7	(6.5)	7.1	(6.9)	7.1	(6.8)
$SiH_2Cl_3^-$						
1	0.0	(0.0)	0.0	(0.0)	0.0	(0.0)
2	3.6	(3.9)	3.5	(3.9)	3.6	(3.9)
3	10.4	(10.3)	10.4	(10.4)	10.5	(10.4)
4	3.7	(4.0)	3.6	(3.9)	3.8	(4.0)
5	14.2	(13.8)	14.1	(13.8)	14.3	(14.0)
6	10.3	(10.2)	10.2	(10.2)	10.5	(10.4)
$SiHF_4^-$						
1	0.0	(0.0)	0.0	(0.0)	0.0	(0.0)
2	4.3	(4.3)	4.1	(4.1)	4.0	(4.0)
3	4.0	(4.1)	4.1	(4.1)	4.0	(4.1)
4	5.0	(4.9)	4.9	(4.8)	4.9	(4.8)
$SiHCl_4^-$						
1	0.0	(0.0)	0.0	(0.0)	0.0	(0.0)
2	2.6	(2.8)	2.5	(2.8)	2.7	(2.9)
3	6.5	(6.6)	6.4	(6.5)	6.6	(6.7)
4	3.7	(3.8)	3.6	(3.8)	3.8	(4.0)
SiF_5^-						
1	0.0	(0.0)	0.0	(0.0)	0.0	(0.0)
2	3.0	(2.9)	3.0	(2.9)	3.0	(2.9)
$SiCl_5^-$						
1	0.0	(0.0)	0.0	(0.0)	0.0	(0.0)
2	3.2	(3.1)	3.1	(3.1)	3.2	(3.2)

[a] The notation level2/basis2//level1/basis1 denotes an energy for level 2 using basis2 at the geometry from basis1 at level1.

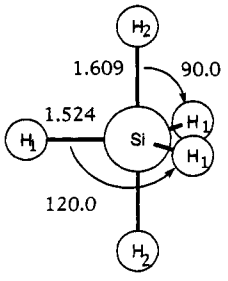

1

D_{3h}

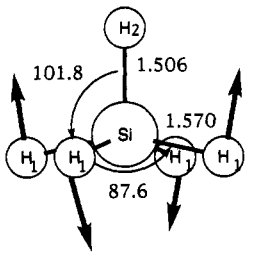

2

C_{4V}, 432i

Figure 1. SiH_5^- MP2/6-31++G(d,p) structures. The imaginary frequency (in cm^{-1}) is given for the transition state.

This type of system has been further explored on the PH_4F surface which displays the same type of topology.[21] The IRCs calculated for the PH_4F system show that the IRC for TS structure **4** leads to a the second TS **2**. The IRC starting from TS **2** leads to the minimum structure **1**. The net effect of this overall pathway is to interconvert two equivalent structures **1** without passing through any other minima.

Several others have explored some of the structures of SiH_4F^-.[2b,c,5,22] Deiter and Holmes[22a,b] (DH) have used RHF/6-31+G(d) to study the two TB structures in the "ideal" Berry

(21) Windus, T. L.; Gordon, M. S. *Theor. Chim. Acta* **1992**, *83*, 21–30.

(22) (a) Deiters, J. A.; Holmes, R. R. *J. Am. Chem. Soc.* **1990**, *112*, 7197–7202. (b) Deiters, J. A.; Holmes, R. R. *J. Am. Chem. Soc.* **1987**, *109*, 1686–1692. (c) Deiters, J. A.; Holmes, R. R.; Holmes, J. M. *J. Am. Chem. Soc.* **1988**, *110*, 7672–7681. (d) Gronert, S.; Glaser, R.; Streitwieser, A. *J. Am. Chem. Soc.* **1989**, *111*, 3111–3117.

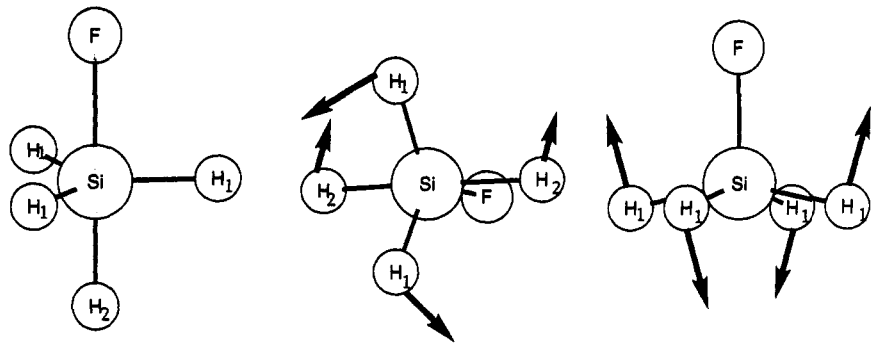

1 2 4

C_{3V} C_{2V}, 194.9i C_{4V}, 797.2i

Figure 2. SiH_4F^- MP2/6-31++G(d,p) structures. Imaginary frequencies (in cm^{-1}) are given for transition states.

Table 3. SiH_4F^- MP2/6-31++G(d,p) Geometries[a]

	1	2	4
Si–F	1.813	1.764	1.692
Si–H_1	1.503	1.526	1.562
Si–H_2	1.575	1.541	
F–Si–H_1	88.4	127.5	101.4
F–Si–H_2	180.0	83.7	
H_1–Si–H_1	119.9	105.0	87.8
H_1–Si–H_2	91.6	93.8	
H_2–Si–H_2		192.6	

[a] Bond lengths in angstroms and angles in degrees.

mechanism. The minimum structure **1** was optimized at the RHF/6-31+G(d) level. The largest difference with our results is an 0.047 Å longer Si–F distance. All other parameters are very similar to those reported here, but no hessians were calculated. In another study,[22c] DH have constrained the angles of the TB "minima" to the idealized angles. Using this method, they found a structure corresponding to the idealized minimum structure **2** which we have characterized as a TS. Again, no hessians were calculated.

Gronert and co-workers[22d] calculated geometries at the RHF/3-21G(d) level for the two TB "minima". The structure for **1** is again very similar to the one reported here, except that the Si–F bond length is longer by 0.063 Å in the present work. There is a reported structure for the "minimum" **2**, however no hessians were calculated. The relative energies of the two isomers were calculated to be 0 and 8 kcal/mol for **1** and **2**, respectively. This is similar to our results of 0.0 and 7.2 kcal/mol for **1** and **2**, respectively.

Gordon and co-workers[2a,b] have also calculated the geometries and energetics of the two "minimum" structures. These were calculated at our level A and, therefore, agree well with our level A results. However, as we have shown,[4] a larger basis set and/or correlation must be used for this system in order to characterize the stationary points correctly. The dissociation limits relative to structure **1** are very similar to those obtained in our previous study.

The studies of Wilhite and Spialter (WS[5]) are compared with our results in Figure 3a. The predictions of WS were obtained using a model in which the electronegative element is modeled by forcing a hydrogen nuclear charge to be +1.1. This gives the hydrogen an electronegativity of 2.9 on the Pauling scale.[23] This is not the electronegativity of hydrogen, fluorine, or chlorine (H, 2.20; F, 3.98; and Cl 3.16). However, it was intended to give a reasonable, qualitative representation of the electronegativity effects (or inductive effects) of a model X.

The plots in Figure 3 are intended to be qualitative. The curvatures shown are obtained using a smoothing algorithm between the points, so they should not be used to infer any actual curvature information. To understand the nature of each structure (i.e. whether it is a minimum or TS), the reader is referred to the figure corresponding to each individual compound.

Our results for SiH_4F^- differ from those of WS (Figure 3a). Nevertheless, using the simple WS model, **3** and **2** are predicted to be quite close in energy and **4** is the highest energy conformer. So, even for this complex system, the WS results provide qualitatively correct information.

SiH_4Cl^-. Structures for this system are given in Figure 4 and the energetics are listed in Table II. Only two of the four possible geometrical isomers were found on this surface. As has been noted in earlier research,[2b,24] chlorine favors an axial or apical position in these pentacoordinated systems. When chlorine is placed in the equatorial or basal positions, the geometry optimization leads either to dissociation of the chlorine from the rest of the molecule or to one of the known structures.

For structure **1**, the Si–Cl bond length is quite long (3.271 Å) compared to that in the SiH_3Cl molecule (2.062 Å). This isomer is bound by a charge-dipole interaction, rather than by strong covalent forces. The Mulliken charge on Cl is –0.9 showing that most of the negative charge lies with Cl. Structure **1** is only 4.6 kcal/mol more stable than $SiH_4 + Cl^-$ and 57.3 kcal/mol more stable than $SiH_3Cl + H^-$, as seen in Table 1.

The TS structure **4** is quite high in energy. At the MP4/6-31++G(d,p)//MP2/6-31++G(d,p) level it is 32.1 kcal/mol relative to structure **1** (Table 2). While structure **4** appears to be the typical Berry TS connecting two equivalent Cl equatorial TB's (see Scheme 2), following the IRC from this TS leads to dissociation of the chlorine anion. This, again, is related to the resistance of chlorine to occupying an equatorial position in the TB structure and is not surprising given that only 4.6 kcal/mol is needed to dissociate Cl^- from structure **1**.

Only a few studies have been performed for the pseudorotation of this system.[2b,5,22] DH have performed optimizations for the two idealized minima by constraining the angles to those of the idealized molecule.[22c] In this fashion, they found a minimum corresponding to the chlorine equatorial in the TB. However, no hessians were performed. Gordon and co-workers[2b] performed level A optimizations for structure **1** and found results that are similar to those in this work with the molecule being described as a charge-dipole complex. They did not find a structure with the chlorine equatorial.

Although SiH_4Cl^- is included in Figure 3a, a comparison of the present work with that of WS is not revealing since two of the necessary structures are not found in the present study.

$SiH_3F_2^-$. The ideal Berry pseudorotation for disubstituted systems is shown in Scheme 3.

(23) (a) Cottrell, T. L.; Sutton, L. E. *Proc. R. Soc., Ser. A* **1951**, *207*, 48. (b) Hurley, A. C. *Proc. R. Soc., Ser. A* **1953**, *218*, 333.

(24) Holmes, R. R. *Pentacoordinated Phosphorus—Structure and Spectroscopy*; American Chemical Society: Washington, DC, 1980; Vol. I, ACS Monograph No. 175.

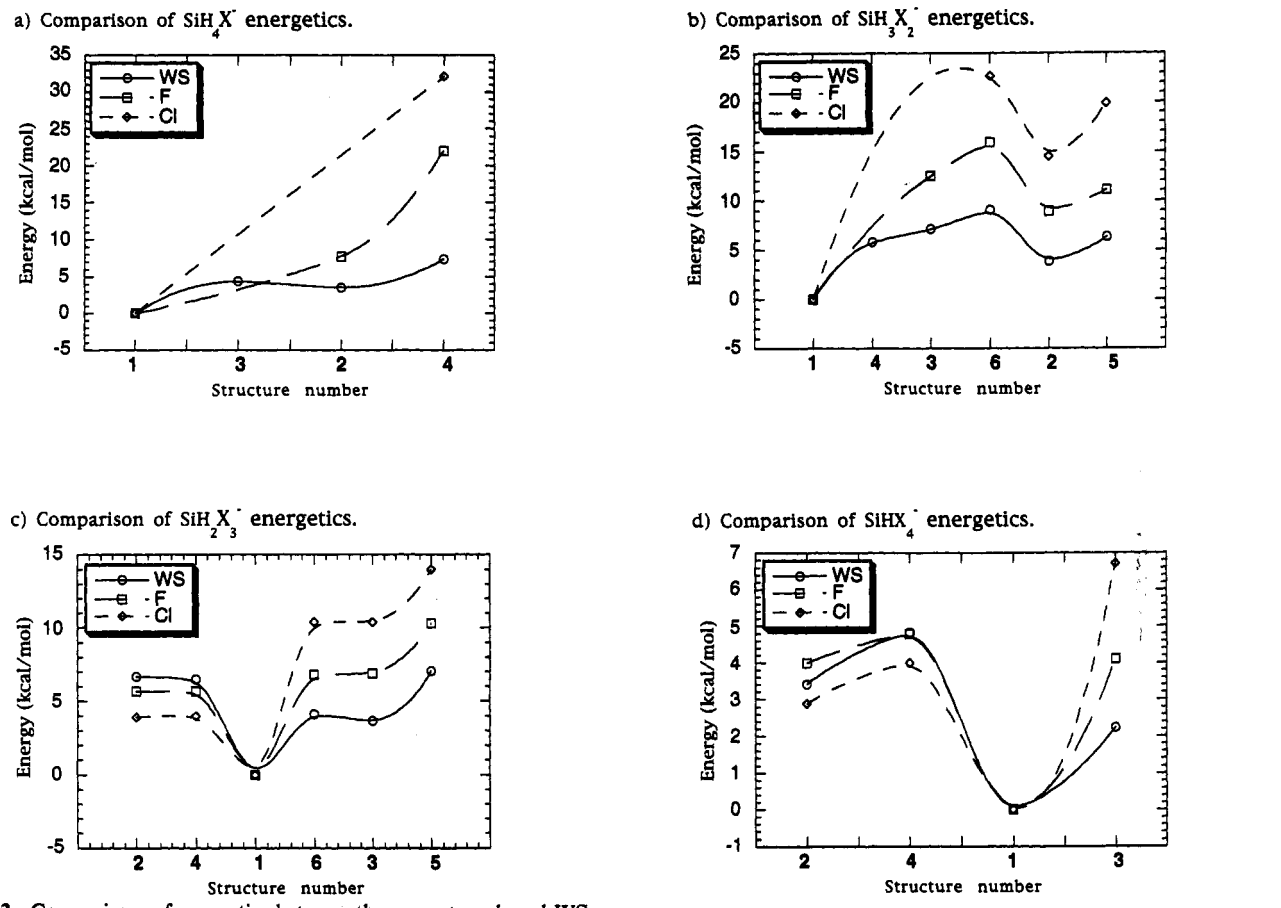

Figure 3. Comparisons of energetics between the present work and WS.

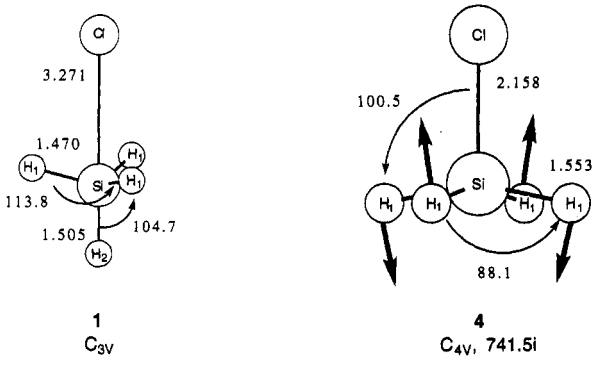

Figure 4. SiH_4Cl^- MP2/6-31++G(d,p) structures. The imaginary frequency (in cm^{-1}) is given for the transition state. Bond lengths are in angstroms and angles are in degrees.

Structures for this system are given in Figure 5 and Table 4 and relative energetics are given in Table 2. All of the structural data are at the C level except that of structure **4**. Despite extensive searches at theory levels B and C, this structure was only found at theory level A. By examining the energetic and geometric differences between **3** and **4** at level A, it is quite easy to see that structures **3** and **4** have coalesced to a distorted minimum (labeled **3** in Figure 5) at higher levels of theory. As an example, the H_1–Si–H_2 angle for structure **3** is 93.2° and the same angle for structure **4** is 94.9° at level A. Also, at MP4/6-31++G(d,p)//RHF/6-31G(d), **3** and **4** have virtually the same energy. The distortions caused by the fluorines seem to cause some structures (**3** and **4** in this case) to coalesce. This is analogous to the results of the SiH_4F^- system. However, this time the coalesced structure (**3** in Figure 5) is a minimum on the surface instead of a transition state.

Since structures **3** and **4** have coalesced to a minimum, there is a question about how structure **1**, the lowest minimum on this

Scheme 3. Ideal Berry Pseudorotation for $SiH_3X_2^-$

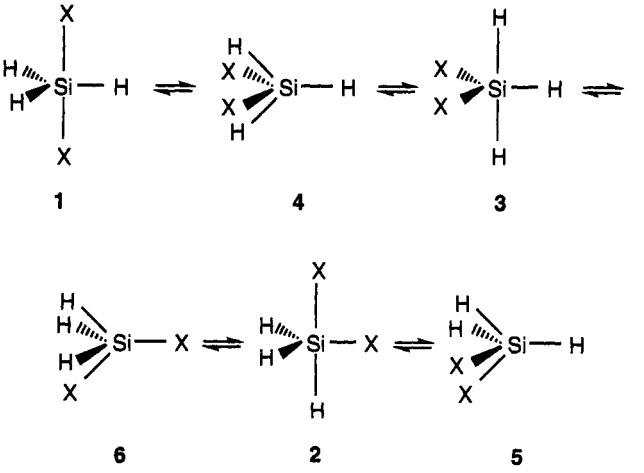

part of the potential energy surface (PES), can isomerize to structure **3**. The most likely possibilities are (a) the existence of a high energy (non-dissociative) route, possibly through a higher order saddle point, or (b) the lack of a non-dissociative route from **1** to **3**.

It is interesting that **5**, with two adjacent fluorines in the base, is only at +11 kcal/mol relative to **1**, whereas in SiH_4F^-, **4** is +22 kcal/mol relative to its minimum. Also, it is interesting that **6**, which can be thought of as a hybrid between **4** in SiH_4F^- and **5** in $SiH_3F_2^-$, is approximately halfway (16 kcal/mol) between the two in energy. So, F seems to prefer the basal to the apical position when given the choice, but prefers TB to SPY even more (i.e. the two coalesce when possible).

All of the previous work for this system has been restricted to the minimum energy structures (**1**–**3**).[2b,5,22a,25] Most of these studies concentrated on the lowest energy minimum structure, **1**.

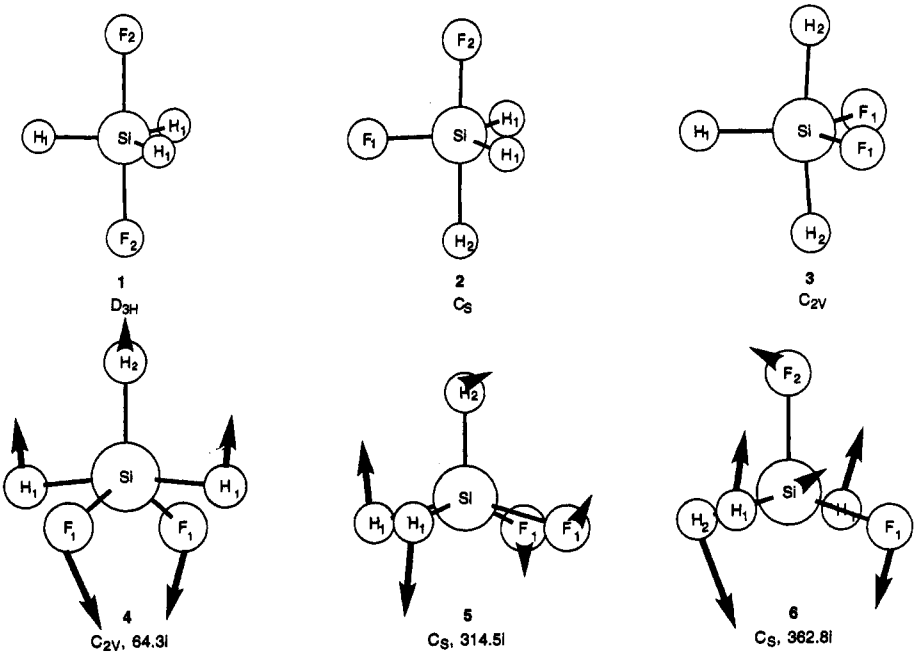

Figure 5. $SiH_3F_2^-$ MP2/6-31++G(d,p) structures. Imaginary frequencies (in cm^{-1}) are given for the transition states. Structure **4** is optimized at the RHF/6-31G(d) level (see text).

Table 4. $SiH_3X_2^-$ MP2/6-31++G(d,p) Geometries[a]

	$SiH_3F_2^-$						$SiH_3Cl_2^-$				
	1	**2**	**3**	**4**[b]	**5**	**6**	**1**	**2**	**4**[b]	**5**	**6**
$Si-X_1$		1.703	1.725	1.673	1.730	1.736		2.081	3.559	2.245	2.306
$Si-X_2$	1.784	1.764				1.685	2.333	3.170	2.118		2.144
$Si-H_1$	1.493	1.504	1.529	1.545	1.535	1.521	1.468	1.462	1.459	1.513	1.495
$Si-H_2$		1.549	1.523	1.527	1.494	1.561		1.496	1.488	1.484	1.547
X_1-Si-X_1			119.9	132.7	87.2					89.1	
X_1-Si-X_2		87.5				106.7		89.7	126.4		110.4
X_1-Si-H_1		121.1	120.0	88.1	86.2	87.3		111.6	60.2	85.1	86.9
X_1-Si-H_2		88.0	88.3	113.6	104.2	149.4		101.5	130.3	102.7	147.8
X_2-Si-X_2	180.0						180.0				
X_2-Si-H_1	90.0	89.0				99.4	90.0	69.5	107.2		99.0
X_2-Si-H_2		175.5				104.0		168.8	103.3		101.8
H_1-Si-H_1	120.0	117.6		170.3	86.2	161.1	120.0	118.8	120.4	88.6	161.9
H_1-Si-H_2		93.4	93.5	94.9	103.1	87.7		105.8	108.7	103.9	88.2
H_2-Si-H_2			173.0								

[a] Bond lengths in angstroms and angles in degrees. [b] This structure is given at the RHF/6-31G(d) level: see text.

Exceptions are the DH study that constrained the isomers to ideal TB angles,[22a] the Fujimoto and co-workers study,[25b,c] and the WS results. As mentioned previously, the DH study included no hessians. Fujimoto and co-workers obtained geometries at our level B and MP4/6-31++G(d,p) energies for structures **1** and **2**. Their geometries and energetics are very similar to the level C calculations presented in this work. All of the calculations relating to structure **1** agree fairly well with the results presented here.

As can be seen in Figure 3b, the model WS results follow our qualitative trends very well. Interestingly, the WS results again show that structures **4** and **3** are very close in energy where the present results show structure **4** to be "missing". This is similar to the WS results for the SiH_4F^- system.

$SiH_3Cl_2^-$. Structures for this system are given in Figure 6 and Table 4 and relative energetics are given in Table 2. All of the structural data are at the C level except that of structure **4** which is at level A. The $Si-Cl_1$ distance of **4** is very long (3.559 Å), and this structure was only found when the C_{2v} symmetry normally associated with this TS was relaxed. This structure did not survive further exploration at levels B and C.

It should be noted that the structure with both chlorines equatorial (**3**) was not found, as would be expected due to the preference of chlorine to bond axially.[24] Optimization of **3** led to **1** with no barrier. The same apical preference very likely explains the absence of structure **4**.

Interestingly, structure **2** disappears at level B but not at levels A and C. Geometry optimizations at level B were performed starting at the optimized structures from both A and C. In each case, Cl_2 (here the subscript refers to atom numbering in Figure 6) tended to dissociate. Even at level C, the $Si-Cl_2$ bond length is quite large (3.170 Å). Still, it is stable to dissociation of Cl^- by 7.2 kcal/mol. The charge on Cl is –0.9, suggesting that **2** is an ion-dipole complex.

By examining the hydrogen bond lengths in the two $SiH_3X_2^-$ systems (Table 4), it is quite clear that the hydrogen bonds in the fluorine-substituted systems are longer than those in the analogous chlorine systems. One explanation for this is that since the fluorines tend to bind more tightly to the silicon than do the chlorines, and since the five bonds in these compounds are formed using just eight electrons (four pairs), the hydrogens must bind less tightly (and therefore lengthen the bond) to compensate. This trend can also be seen in the SiH_4X^- system, but the comparison is not as clear here, since the chlorine system is missing

(25) (a) Magnusson, E. *J. Am. Chem. Soc.* **1993**, *115*, 1051–1061. (b) Fujimoto, H.; Yabuki, T.; Tamao, K.; Fukei, K. *THEOCHEM* **1992**, *92*, 47–61. (c) Fujimoto, H.; Arita, N.; Tamao, K. *Organometallics* **1992**, *11*, 3035–3041.

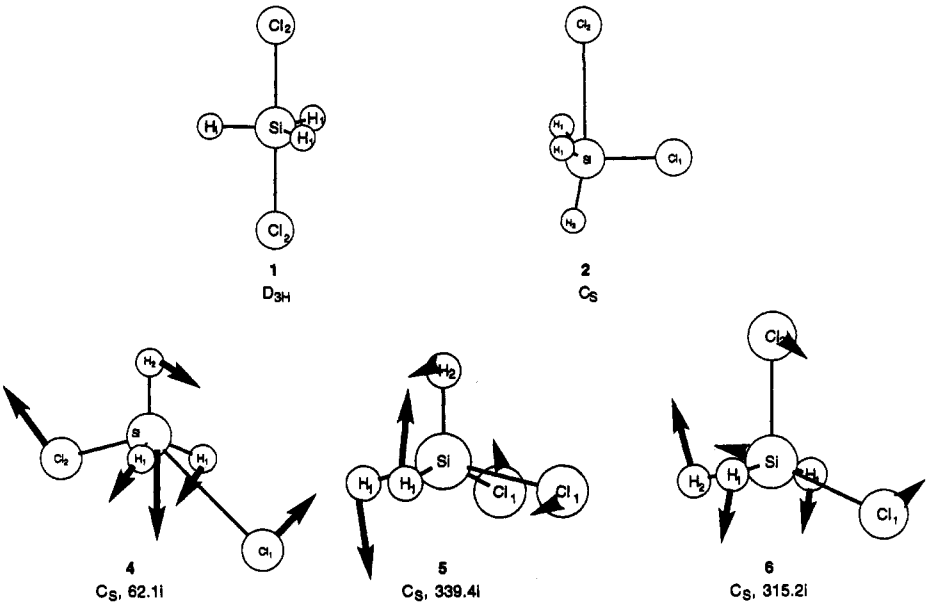

Figure 6. $SiH_3Cl_2^-$ MP2/6-31++G(d,p) structures. Imaginary frequencies (in cm^{-1}) are given for the transition states. Structure **4** is optimized at the RHF/6-31G(d,p) level (see text).

two of the structures, the minimum (**1**) is a charge-dipole complex, and the transition state structure (**4**) is above the Cl^- dissociation limit.

The energy of the TS structure **6** relative to **1** is above the limit for Cl^- dissociation from **1** by about 1 kcal/mol. The IRCs for this structure show that **6** is indeed a TS associated with structure **2** in one direction (this is the direction shown in Figure 6). However, in the other direction (that would lead to structure **3** in the classical Berry pseudorotation: see Scheme 3) the IRC instead leads to dissociation of Cl^-. This clearly illustrates the instability of chlorine when it is equatorial. This also suggests that there may be a slight barrier of 1.0 kcal/mol for the more or less on edge attack of Cl^- on SiH_3Cl.

Transition state structure **5** is only slightly below the Cl^- dissociation limit from **1** (1.8 kcal/mol). An IRC calculation shows that **5** is the transition state structure connecting two equivalent **2**s. However, even this result is slightly different from that proposed by Berry. There is large "precessional motion" of H_2 and Si (refer to Figure 6) that is not generally associated with Berry pseudorotation. This "motion" is largely associated with the closing (or opening in the direction opposite to that shown) of the H_2–Si–H_1 angle. However, the end results are the same. Further examples of this behavior are presented below.

The only previous calculations known for this system were performed on the three minima.[2b,22a] The study by DH again assumes ideal angles for the TB structures. This works well for structure **1** but is obviously not correct for structures **2** and **3**. The study of Damrauer and co-workers[2b] is at our theory level A and only for structure **1**. The limit for dissociation of Cl^- is essentially identical to the results presented here.

The results of WS (in Figure 3b) again follow the trend of the present results with the exception of structures **3** and **4**. One might expect that the behavior predicted by the WS model would be closer to our chlorine predictions than those of fluorine, since the electronegativity of the WS model (2.9) is much closer to that of chlorine than fluorine. However, chlorine is much larger than fluorine and therefore should show appreciable steric effects. This is, no doubt, the reason for chlorine not having many of the typical isomers of these systems. Another contributing factor is that the Si–F bond is also much stronger than the Si–Cl bond, so Si–Cl is floppier and easier to dissociate.

$SiH_2F_3^-$. The ideal Berry pseudorotation pathway for trisubstituted systems is given in Scheme 4.

Geometries for this system are given in Figure 7 and Table 5 and relative energetics are given in Table 2. All of the structural

Scheme 4. Ideal Berry Pseudorotation Pathway for $SiH_2X_3^-$

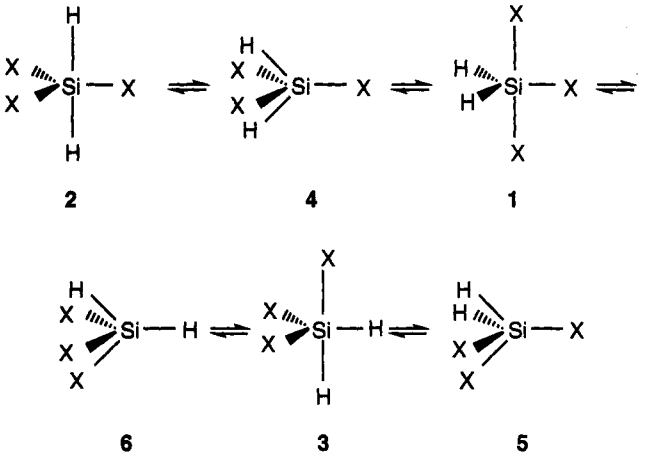

data are at the C level. This is the first system (other than SiH_5^-) where all of the classically expected structures are found at the highest level of theory. All of the geometric parameters are fairly normal with no great surprises. This may account for finding all six of the structures at level C. However, note that at the highest level of theory, including zero-point vibrational energies, the energy of **4**, the TS connecting **1** and **2**, is identical to that of **2**, so these two structures could well coelesce at even higher levels of theory. The same may be said for **6** and **3**.

IRCs from the TSs verify that the Berry pseudorotation mechanism is indeed followed for this system. As was seen in the $SiH_3Cl_2^-$ system, the normal modes for **5** and **6** show a "precessional motion" where the F_2 for **5** and H_2 for **6** are involved in decreasing (or increasing) bond angles. Even the silicon centers of these molecules participate in this "motion".

The energies of all $SiH_2F_3^-$ isomers are much lower relative to **1** than are those in the SiH_4F^- system. They are also lower in energy relative to **1** than are the isomers in $SiH_3F_2^-$ relative to its lowest isomer. Indeed, the energies seem to cluster closer together with increasing heavy atom substitution.

The only previous calculations for $SiH_2F_3^-$ were performed by DH[22a,b] and WS. DH examined only the minima (**1**–**3**), and since the TB structures are not very distorted from the ideal, the DH model of constraining the angles works fairly well for this system. Their relative energies are within 1 kcal/mol of those presented here. In another study, DH have minimized structure

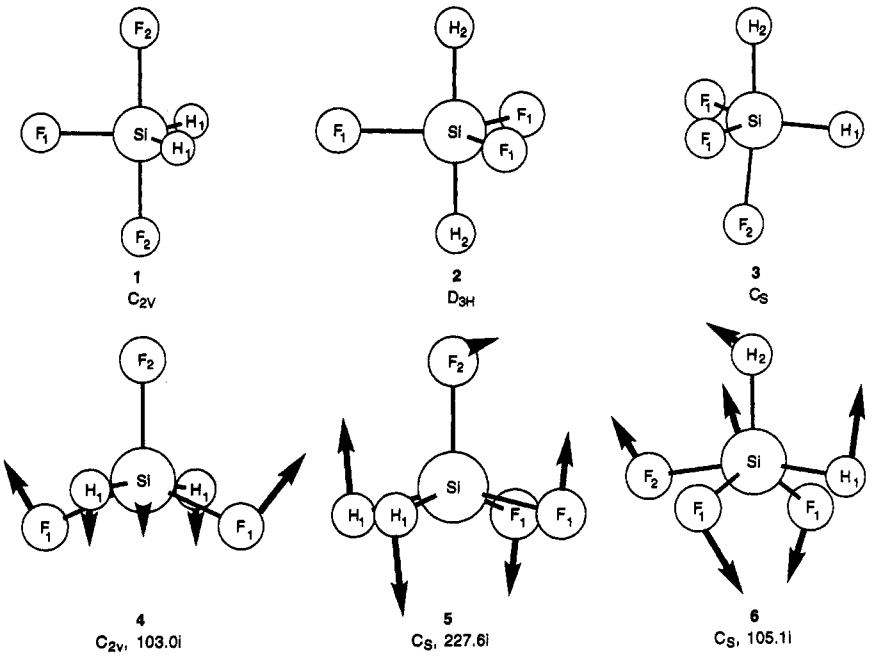

Figure 7. $SiH_2F_3^-$ MP2/6-31++G(d,p) structures. Imaginary frequencies (in cm^{-1}) are given for transition states.

Table 5. $SiH_2X_3^-$ MP2/6-31++G(d,p) Geometries[a]

	$SiH_2F_3^-$						$SiH_2Cl_3^-$					
	1	**2**	**3**	**4**	**5**	**6**	**1**	**2**	**3**	**4**	**5**	**6**
$Si-X_1$	1.674	1.714	1.695	1.728	1.717	1.712	2.099	2.198	2.158	2.232	2.230	2.183
$Si-X_2$	1.749		1.728	1.691	1.667	1.717	2.291		2.271	2.149	2.114	2.239
$Si-H_1$	1.487		1.501	1.497	1.521	1.516	1.465		1.485	1.472	1.498	1.492
$Si-H_2$		1.498	1.523			1.493		1.473	1.497			1.483
X_1-Si-X_1		120.0	123.8	135.5	86.0	137.5		120.0	125.4	133.7	87.0	134.3
X_1-Si-X_2	90.9		88.1	112.2	101.6	87.0	94.2		89.0	113.2	102.8	88.5
X_1-Si-H_1	116.9		118.0	88.1	85.7	87.3	114.9		117.2	87.8	84.5	87.0
X_1-Si-H_2		90.0	88.9			111.2		90.0	88.5			112.8
X_2-Si-X_2	179.2						171.6					
X_2-Si-H_1	89.6		89.8	95.0	103.2	164.4	88.2		87.9	95.5	102.1	168.4
X_2-Si-H_2			173.8			94.7			174.4			91.4
H_1-Si-H_1	126.1			170.0	92.1		130.3			169.0	93.4	
H_1-Si-H_2			96.3			100.9			97.7			100.2
H_2-Si-H_2		180.0						180.0				

[a] Bond lengths in angstroms and angles in degrees.

1,[22a] and those predictions agree well with the current results (bond lengths agree to within 0.04 Å and angles agree to within 1°).

The predictions of the WS model (Figure 3c) are in reasonably good qualitative agreement with the more accurate calculations presented here. The main difference is the relative energetics of structures **6**, **3**, and **5** compared to **2** and **4**. It appears that the qualitative model is unable to reproduce the effects of moderate distortions, such as those predicted for structures of **6**, **3**, and **5** in the present work.

$SiH_2Cl_3^-$. Geometries for this system are given in Figure 8 and Table 5 and relative energetics are given in Table 2. All of the structural data are at the C level. Interestingly, all of the classically expected structures for this system are found, and there are no long Si–Cl bonds as in the SiH_4Cl^- and $SiH_3Cl_2^-$ systems. Another interesting trend (shown in Table 5) is that the angles in $SiH_2Cl_3^-$ are very similar to those in $SiH_2F_3^-$. The largest discrepancies are for the **1** isomers. There is quite a bit of distortion of the axial chlorines from linear ($Cl_2-Si-Cl_2$ = 171.6°). This can be attributed to the large size of the chlorines. As in $SiH_3X_2^-$, the hydrogen bonds of the fluorine-substituted system are longer than those of the analogous chlorine system.

The relative energies of all six structures are fairly low and are much lower than the Cl^- dissociation limit relative to **1**. As already noted for $SiH_2F_3^-$, structures **2** and **4** and structures **3** and **6** are very similar in energy and therefore each pair may ultimately coalesce. This is very easy to understand since the geometries are also very similar. The energetics are also clustering closer together for this system than those for the $SiH_3Cl_2^-$ and SiH_4Cl^- systems. This is the same trend seen for the fluorine-substituted systems.

IRC calculations confirm that the Berry pseudorotation mechanism is essentially followed in $SiH_2Cl_3^-$. Interestingly, the normal modes for **5** and **6** show large "motions" of Cl_2 (**5**), H_2 (**6**), and Si. These are the same type of "motions" that are seen in structures **5** and **6** of $SiH_2F_3^-$.

The only previous calculations of this system are those of DH[22a] and WS. Because the minima are not distorted very much from the ideal TB structure, the constrained results of DH give good relative energetics for the three minima, agreeing with the fully optimized results to within 2 kcal/mol for structure **2** and ~0 kcal/mol for structure **3**.

The comparison of the present work with that of WS is given in Figure 3c. Our chlorine results suggest an even bigger differential between the energies of structures **6**, **3**, and **5** relative to those of structures **2** and **4** than is found for fluorine. As noted above, this is due to steric effects of the chlorine and the different strengths of Si–F and Si–Cl bonds.

$SiHF_4^-$. The idealized Berry pseudorotation for tetrasubstituted systems is given in Scheme 5.

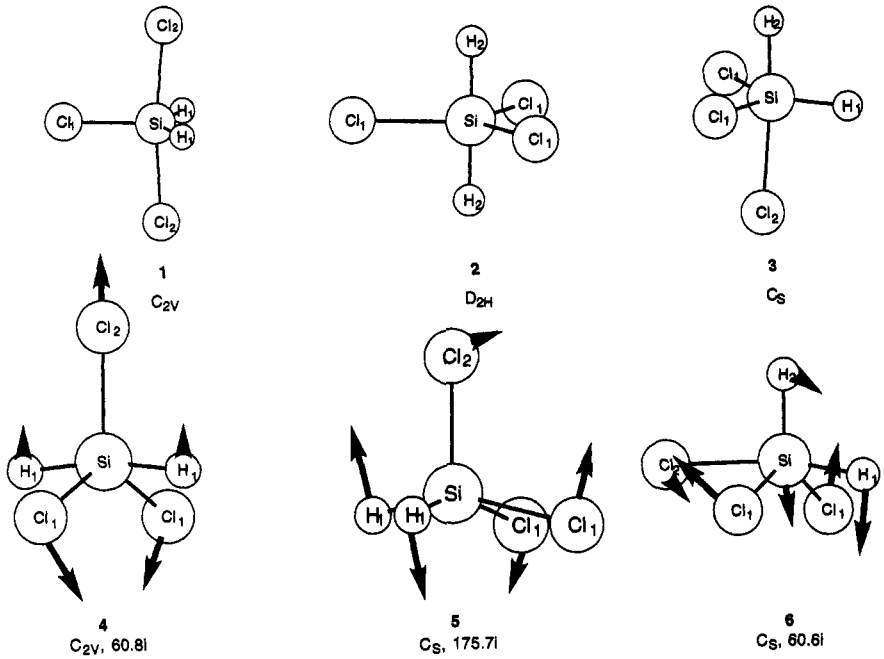

Figure 8. $SiH_2Cl_3^-$ MP2/6-31++G(d,p) structures. Imaginary frequencies (in cm^{-1}) are given for transition states.

Scheme 5. Idealized Berry Pseudorotation for $SiHX_4^-$

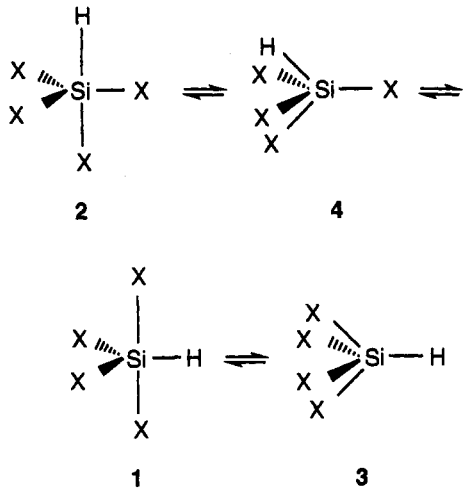

Structures for this system, which is the inverse of SiH_4F^-, are given in Figure 9 and Table 6 and relative energetics are given in Table 2. All of the structural data are at the C level. The four structures are not distorted very much from their "ideal" structures. Relative energies are even smaller and more tightly clustered in this system than the previous fluorine-substituted systems.

IRC calculations verify the Berry pseudorotation mechanism for this system. However, there is again additional "motion" in **4** that is not predicted by the Berry mechanism.

DH[22b] and WS provide the only previous calculations for $SiHF_4^-$. The relative energetics of the DH study are in excellent agreement with ours (differing by 0.1 kcal/mol) for the two minima.

The comparison with the WS results in Figure 3d shows good relative agreement between the two methods. Our results for **3** are high energetically compared to the WS results, but the overall relative energies generally compare well. Also, note that in all cases, the WS model predicts a smaller energy variation than is actually found until $SiHX_4^-$.

$SiHCl_4^-$. Structures for this system are given in Figure 10 and Table 6 and relative energies are given in Table 2. All of the structural data are at the C level. As in the $SiH_2Cl_3^-$, there are

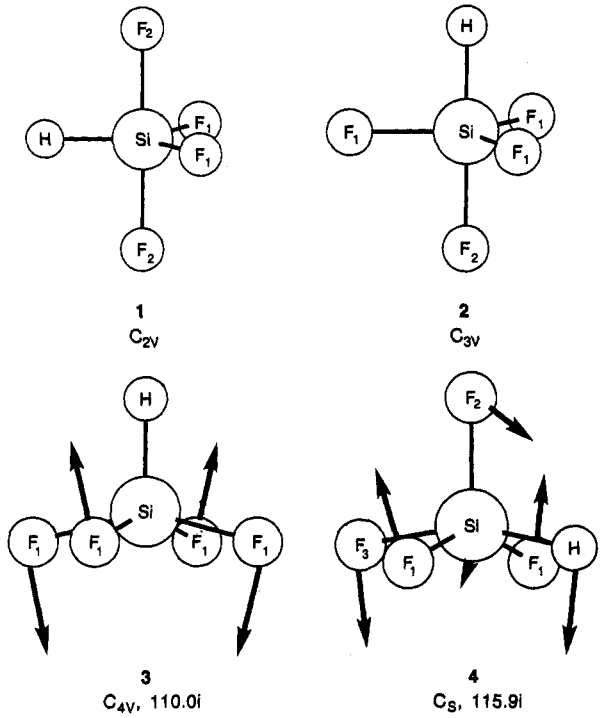

Figure 9. $SiHF_4^-$ MP2/6-31++G(d,p) structures. Imaginary frequencies (in cm^{-1}) are given for transition states.

no long Si–Cl bonds. The angles for this system are very close to those of the associated $SiHF_4^-$ system. Again, the largest difference occurs for the X_2–Si–X_2 angles which are ideally linear in the structures numbered **1**. Also, the hydrogen bond distances in $SiH_2F_3^-$ are consistently longer than those associated with $SiH_2Cl_3^-$.

The Berry pseudorotational mechanism is followed for this compound. Again, there is additional "motion" of Cl_2 and Si associated with **4** that is not predicted by the Berry mechanism. This has been a common thread among the species that are not fully substituted by the same ligand. Therefore, we propose a fine-tuning of the Berry mechanism in those cases for which the basal ligands are not the same. Then there is additional "motion" of the apical ligand in the SPY TS and possibly the central atom (silicon in this case). This does not occur, of course, when such

Table 6. $SiHX_4^-$ MP2/6-31++G(d,p) Geometries[a]

	$SiHF_4^-$				$SiHCl_4^-$			
	1	**2**	**3**	**4**	**1**	**2**	**3**	**4**
$Si-X_1$	1.664	1.683	1.699	1.703	2.100	2.151	2.185	2.204
$Si-X_2$	1.720	1.699		1.659	2.254	2.194		2.107
$Si-X_3$				1.691				2.162
Si–H	1.481	1.498	1.473	1.495	1.466	1.479	1.468	1.474
X_1-Si-X_1	115.3	120.0	86.8	144.3	114.6	120.0	87.4	145.7
X_1-Si-X_2	90.3	89.2		107.8	91.7	90.6		107.1
X_1-Si-X_3				87.2				88.8
X_1–Si–H	122.4	90.8	103.8	87.7	122.7	89.4	102.4	85.8
X_2-Si-X_2	179.0				173.6			
X_2-Si-X_3				96.7				99.0
X_2–Si–H	89.5	180.0		99.7	86.8	180.0		99.6
X_3–Si–H				163.6				161.5

[a] Bond lengths in angstroms and angles in degrees.

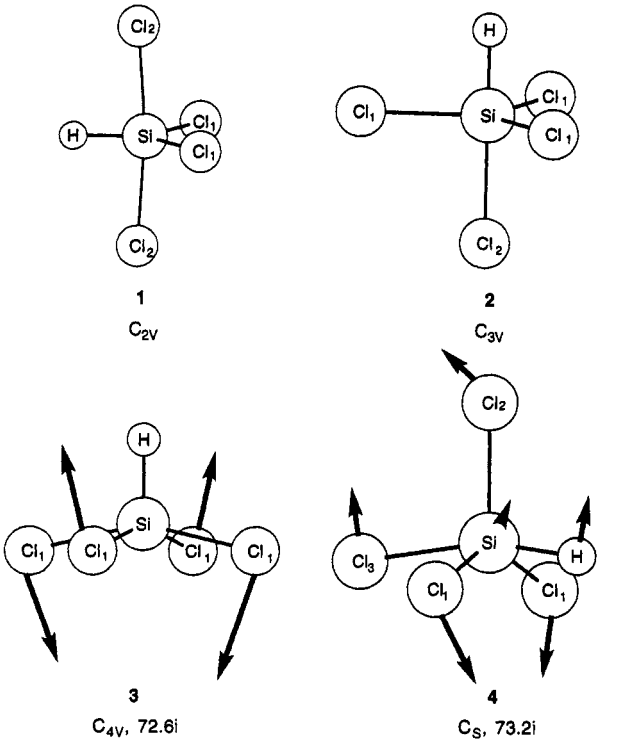

Figure 10. $SiHCl_4^-$ MP2/6-31++G(d,p) structures. Imaginary frequencies (in cm^{-1}) are given for transition states.

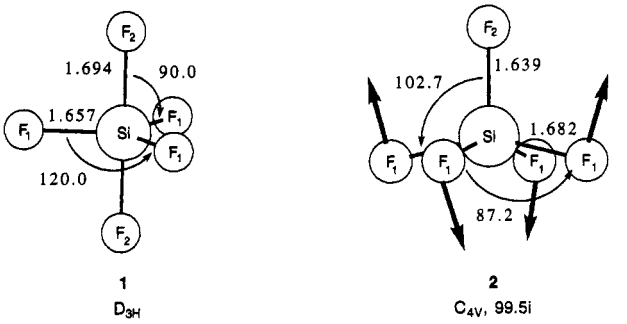

Figure 11. SiF_5^- MP2/6-31++G(d,p) structures. The imaginary frequency (in cm^{-1}) is given for the transition state. Both lengths are in angstroms and angles are in degrees.

motions are precluded by symmetry. Indeed the Berry mechanism presumes a degree of symmetry that precludes this "precessing" motion.

DH[22b] and WS provide the only previous computational results for $SiHCl_4^-$. DH predict **2** to be 2.2 kcal/mol higher in energy than we do.

Again, the comparison with the WS results (Figure 3d) appears to be fairly good. The one major difference is the relative energy of **3**. This may be related to the distortion of Cl_3 from the "ideal" structure. The bond length of Si–Cl_3 of 2.162 Å is about 0.04 Å longer than that of Si–Cl_1 and the Cl_2–Si–Cl_3 bond angle is about 8° smaller than that of Cl_2–Si–Cl_1.

SiF_5^-. Structures for this system are given in Figure 11 and relative energetics are given in Table 2. All of the structural data are at the C level. The results are similar to those discussed earlier for SiH_5^- (Scheme 1). Even the energetics of the two systems are similar, with an energy barrier of 2.2 and 2.9 kcal/mol for the SiH_5^- and SiF_5^- pseudorotational mechanisms, respectively. The trends in bond lengths are also similar for the two systems with $Si-X_{axial} > Si-X_{apical} > Si-X_{basal} > Si-X_{equatorial}$. One of the major differences between the two systems is the X^- dissociation limit. The addition of F^- to SiF_4 is exothermic by 72.3 kcal/mol (Table 1), whereas the addition of H^- to SiH_4 is exothermic by only 15.8 kcal/mol.

An IRC calculation tracking the path from **2** to **1** verifies the Berry pseudorotational mechanism.

Many experimental studies have been performed on this SiF_5^- anion,[26] with several of them relating to the exchange mechanism of F^- in several different solutions.[26a-d] The anion has been observed in ion cyclotron resonance (ICR) experiments[26e-i] in small quantities. The F^- dissociation is estimated to be 60 ± 4 kcal/mol relative to **1**. This is approximately 12 kcal/mol less than the dissociation limit predicted in this study. IR and Raman studies have been performed in an argon matrix[26j,k] and in aqueous solution.[26l,m] The heat of formation has been determined to be less than or equal to −583 kcal/mol[26n] and relaxation times as a function of temperature have been determined.[26e] One X-ray structure has been determined for the $[(phenyl)CH_2N(methyl)_3]$-$[SiF_5]$ salt.[26o] The largest deviation from TB for the anion was the F_{eq}–Si–F_{eq} angle (117.5°). Thermally corrected values of the bond lengths are 1.660 and 1.622 Å for Si–F_{ax} and Si–F_{eq}, respectively. These correspond to the MP2/6-31++G(d,p) bond lengths of 1.694 and 1.657 Å for the Si–F_2 and Si–F_1 bond lengths of the free anion. This agreement is very good considering the amount of distortion observed in the crystal structure.

Several theoretical studies have been performed that relate to SiF_5^-.[5,22a,27] The ionization potential (IP) has been calculated

(26) (a) Gel'mbol'dt, V. O. *Koord. Khim.* **1989**, *15*, 1501–1503. (b) Marat, R. K.; Janzen, A. F. *Can. J. Chem.* **1977**, *55*, 3845–3849. (c) Gibson, J. A.; Ibbott, D. G.; Janzen, A. F. *Can. J. Chem.* **1973**, *51*, 3203–3210. (d) Parpiev, N. A.; Maslennikov, I. A. *Usb. Khim. Zh.* **1968**, *12*, 6–9. (e) Reynhardt, E. C.; Froneman, S. *J. Magn. Reson.* **1988**, *80*, 268–279. (f) Saes, L. H.; Brongersma, H. H.; Van d'Hart, W. J. *Symp. Proc. Int. Symp. Plasma Chem., 7th* **1985**, *4*, 1355–1359. (g) Larsen, J. W.; McMahon, T. B. *J. Am. Chem. Soc.* **1985**, *107*, 766. (h) Larsen, J. W.; McMahon, T. B. *J. Am. Chem. Soc.* **1983**, *105*, 2944. (i) Larsen, J. W.; McMahon, T. B. *J. Am. Chem. Soc.* **1982**, *104*, 5848. (j) Jacox, M. E. *J. Phys. Chem. Ref. Data* **1984**, *13*, 945–1068. (k) Ault, B. S. *Inorg. Chem.* **1979**, *18*, 3339. (l) Kleboth, K. *Montash. Chem.* **1970**, *101*, 357–361. (m) Kleboth, K. *Montash. Chem.* **1968**, *99*, 1177–1185. (n) Thynne, J. C. J.; MacNeil, K. A. G. *Inorg. Chem.* **1970**, *9*, 1946–1947. (o) Schomburg, D.; Krebs, R. *Inorg. Chem.* **1984**, *23*, 1378.

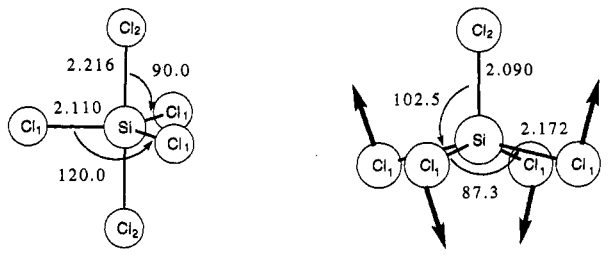

Figure 12. $SiCl_5^-$ MP2/6-31++G(d,p) structures. The imaginary frequency (in cm^{-1}) is given for the transition state. Bond lengths are in angstroms and angles are in degrees.

using Xα theory;[27a,b] the dissociation of F^- has been studied by several workers;[27c-e] and the reaction $SiF_5^- + F^- \rightarrow SiF_6^{2-}$ has been studied using coupled Hartree–Fock perturbation theory (CHFPT) with a near Hartree–Fock limit basis set[27f] and using RHF/6-31++G(d,p) theory.[2b] Each of these studies only examined the minimum structure (**1**). All of the studies produced geometries that were 0.03–0.04 Å different in the bond lengths than those presented here. WS predicted a pseudorotation barrier of 2.94 kcal/mol which is in excellent agreement with our results. The calculated F^- dissociation energies agree to within 6 kcal/mol of our results. Interestingly, all the other calculated dissociation energies were higher than those presented here, even though the estimated experimental dissociation energy is approximately 12 kcal/mol lower than that predicted here.

$SiCl_5^-$. Structures for this system are given in Figure 12 and relative energetics are given in Table 2. All of the structural data are at the C level.

Most of the comments regarding SiF_5^- apply to this system as well. The same trend is found in bond lengths and energetics: the largest difference between this system and SiH_5^- and SiF_5^- is the dissociation energy. The exothermicity of Cl^- reacting with $SiCl_4$ (21.9 kcal/mol) is much closer to that of SiH_5^- (15.8 kcal/mol) than SiF_5^- (72.3 kcal/mol). This reflects the relative strengths of Si–Cl vs Si–F bonds in these complexes.

An IRC calculation verifies the Berry mechanism for this system. Interestingly, the trend from monosubstitution to pentasubstitution of heavy atoms seem to be a stabilizing one. The more heavy elements (compared to H) that are present the more likely the system is to have all of the isomers predicted by the Berry model and the smaller the relative energetics are compared to the local minimum.

Several experiments have succeeded in finding evidence of $SiCl_5^-$.[28a,c] The compound has been observed spectroscopically in a solution of $(CH_3)NO_2$.[28a] It has also been investigated in an electron attachment study of tetrachlorosilane.[28c] Two groups have performed ICR experiments in an attempt to find evidence for the $SiCl_5^-$ anion with no success.[28b,26g] In the study by Sheldon and co-workers,[28b] an SCF/6-21G optimization and hessian was performed, verifying that the TB structure was a minimum. Using these results, they had hoped to successfully produce the anion, but their attempts were not successful.

The only other theoretical studies of $SiCl_5^-$ were Xα calculations of the electron attachment of $SiCl_5$,[27a,b] and the WS paper. The structure used for **1** in the Xα studies had bond lengths of 2.13 and 2.08 Å for the $Si–Cl_2$ and $Si–Cl_1$ bond distances, respectively. The $Si–Cl_2$ distance is quite different from that predicted in our work (2.216 Å). As mentioned in the SiF_5^- section, the WS relative energies are very similar to those presented here (0.3 kcal/mol difference for the relative energy of **2**).

Summary of Energetics

Addition of F^- to silane is exothermic by more than 30 kcal/mol, while the addition of a chloride ion only reduces the energy by 4.6 kcal/mol. This reflects the fact that SiH_4F^- is a true trigonal-bipyramidal structure, whereas SiH_4Cl^- is a weakly bound ion-dipole complex. Because a second Cl (in $SiH_3Cl_2^-$) occupies an axial position opposite the first Cl, the lowest energy arrangement of $SiH_3Cl_2^-$ is much more stable relative to $SiH_3Cl + Cl^-$ than is SiH_4Cl^- relative to dissociation of Cl^-. Interestingly, the dissociation of $SiH_nCl_{5-n}^- \rightarrow SiH_nCl_{4-n} + Cl^-$ is nearly constant for $n \leq 3$, as shown in Table 1. In contrast, the corresponding dissociations of $SiH_nF_{5-n}^-$ became monotonically more endothermic as n decreases.

Relative to X^- dissociation (X = H, F, Cl), the pseudorotation PES is much less demanding energetically for SiH_5^-, $SiH_3F_2^-$, $SiH_2X_3^-$, $SiHX_4^-$, and SiX_5^-. Indeed, the pseudorotation barriers for SiH_5^-, SiF_5^-, and $SiCl_5^-$ are all ≤3 kcal/mol.

Conclusions

There are several general conclusions that can be drawn from this work.

(1) There seems to be a trend that the more heavy elements (compared to H) that are substituted on the silicon the closer the potential energy surface is to an idealized Berry surface; that is the highly substituted structures do not distort very much from the ideal TB or SPY configuration. Also, structures that are expected in the Berry model tend to be found in highly substituted systems.

The highly substituted systems also seem to have lower relative energies that are clustered closer together than the less substituted systems. Therefore, they have lower pseudorotational barriers, and all of the minima on the surface should be easily accessible. They also have isomers and pseudorotation barriers that are much lower in energy than the dissociation limits.

(2) The simple electronegativity model proposed by Wilhite and Spialter gives generally good results when compared to the accurate calculations presented here. The greatest differences arise for those structures that have large distortions (generally associated with size) from the "ideal" Berry model. This agreement is remarkable considering the time at which the WS calculations were performed and their simplified nature.

(3) The systems that have all of the same ligands (i.e. SiX_5^-) have bond lengths that follow the trend $Si–X_{axial} > Si–S_{apical} > Si–X_{basal} > Si–X_{equatorial}$.

(4) The hydrogen bond distances in a particular $SiH_{5-n}X_n^-$ (n = 1–4) system are consistently longer in the fluorine-substituted systems than in the analogous chlorine systems. This is believed to be related to the tighter binding of the fluorines to the silicon which in turn induces a "loosening" of the hydrogen binding and therefore lengthens the hydrogen bond.

(5) Much of the information presented here may be useful in determining S_N2 reaction mechanisms. However, since most of the structures lie below the X^- dissociation limits, only dynamics calculations will be able to determine how much energy for the initial $SiY_{4-n}X_n + X^-$ reaction can be transferred in the pseudorotational motion.

(6) We have calculated IRCs for the transition states to verify the minima associated with them. In many cases these led to the expected minima on the Berry pseudorotational path, but occasionally these led to dissociation. Where there is asymmetry in the ligands of a TS, we have found a "precessional motion"

(27) (a) Gutsev, G. L.; Boldyrev, A. I. *Zh. Neorg. Khim.* **1981**, *26*, 2353–2357. (b) Gutsev. G. L.; Boldyrev, A. I. *Chem. Phys.* **1981**, *56*, 277–283. (c) Sliznev, V. V.; Solomonik, V. G. *Mol. Strukt.* **1990**, 38–47. (d) Gel'mbol'dt, V. O. *Zh. Neorg. Khim.* **1989**, *34*, 231–232. (e) O'Keefe, M. *J. Am. Chem. Soc.* **1986**, *108*, 4341–3. (f) Kleboth, K.; Rode, B. M. *Montash. Chem.* **1974**, *105*, 815–821. (g) Tossell, J. A.; Lazzeretti, P. *J. Chem. Phys.* **1986**, *84*, 369–374. (h) Gutsev, G. L. *J. Chem. Phys.* **1993**, *99*, 3906–3912.

(28) (a) Beattie, I. R.; Livingston, K. M. S. *J. Chem. Soc. A* **1969**, *5*, 859–860. (b) Sheldon, J. C.; Hayes, R. N.; Bowie, J. H. *J. Am. Chem. Soc.* **1984**, *106*, 7711–7715. (c) Moylan, C. R.; Christopher, R.; Green, S. B.; Brauman, J. I. *Int. J. Mass Spectrom. Ion Processes* **1990**, *96*, 299–307.

that is not expected in the traditional Berry mechanism and suggest that this type of motion be used as a "fine-tuning" of the mechanism.

Acknowledgment. The calculations in this work were performed on an IBM 3090/200E computer at North Dakota State University Computer Center, obtained in part with a joint study agreement with IBM, the Cray Y-MP at the San Diego Supercomputer Center, and RS/6000s provided by Iowa State University. Funding was provided from the Air Force Office of Scientific Research (92-0226) and a GAANN fellowship from the Department of Education to T.L.W.

Supplementary Material Available: Structural information for the reactants, Mulliken populations, and frequencies (4 pages). This material is contained in many libraries on microfiche, immediately follows this article in the microfilm version of the journal, and can be ordered from the ACS; see any current masthead page for ordering information.